



Anti-erosive Boron and Fluorine Doped Polyimide Coatings for Space Radiation Environment Protection

Riyadh MA Abdul Majeed¹, Prashant S Alegaonkar^{2*}, Sudha V Bhoraskar³ and Vasant N Bhoraskar³

¹Department of Physics, University of Hodaidah, Hodaidah, Yemen

²Department of Physics, School of Basic Sciences, Central University of Punjab, Bathinda, PS, India

³Department of Physics, University of Pune, Ganeshkhind, Pune, MS, India

*Corresponding Author: Prashant S Alegaonkar, Department of Physics, School of Basic Sciences, Central University of Punjab, Bathinda, PS, India.

Received: December 13, 2022

Published: December 20, 2022

© All rights are reserved by Prashant S Alegaonkar., et al.

Abstract

Radiation resistant coatings are of utmost importance for the space vehicle protection. Herein, we report on radiation assisted doping of boron and fluorine (B/F) in polyimide ($C_{22}H_{10}N_2O_5$, PMDA-ODA, Kapton-H) to enhance the erosion resistant capability against atomic oxygen (AO) ions. Doping of B/F in polyimide is carried out using Co-60 γ -radiations over a dose range of 64-384 kGy@room temperature. Boron is seen to be distributed at a depth of $\sim 2 \mu\text{m}$ from the surface, whereas fluorine is bonded to carbonaceous backbone. Details of the bonding architecture is presented. Virgin and B/F polyimide are subjected to AO ions from plasma having an average energy of $\sim 12 \text{ eV}$, and fluence over $5\text{-}20 \times 10^{16} \text{ ions/cm}^2$. The paper reports the analysis of the mass loss, erosion characteristics, modifications in surface texture apart from the molecular and electronic properties. By and large it is observed that the mass loss is prevented by three-fold times, wherein, erosion yield is reduced by a factor of two in B/F polyimide (@max. doping) as compared to that in the virgin. Effectively, the presence of boron and C-F bonding offers erosion resistance to polyimide by AO ions. Similar improvement in the radiation resistance for polyimide is expected for atomic oxygen. Details are presented.

Keywords: Atomic Oxygen; Plasma Treatment; Polyimide; Surface Modifications; Radiation Resistance

Introduction

During the recent years, there is a rise in the space mission programs activated through the launching of satellites for navigation, communication, purpose and weather studies. Moreover, there is an emerging trend of launching shuttle vehicles in shallow space for business travel destination [1]. Consequently, this has put forward a demand in the area of space research and development to design satellites and, particularly, earth re-entry space vehicles with improved radiation and thermal protection systems [2].

In general, such space vehicles are designed to operate into two types of earth's atmospheric conditions: (a) low earth orbits (LEO, 200-700 km altitude above the mean sea level) and (b) geosyn-

chronous (36000 km) orbits [3,4]. Particularly, LEO vehicles experience rather turbulent and arid space environment. These are comprised of high vacuum, thermal variations, exposure to solar and far ultraviolet radiations as well as impact by meteoroids and debris. In addition, there are trapped charge particles such as electrons, protons, and atomic oxygen from plasma, and other neutral and reactive species [5-7]. These can affect the performance of radiation protection systems. By and large, these factors deteriorate the performance parameters in terms of initial physicochemical, mechanical, optical, thermal, and other overall lifetime of protection system and, ultimately, lead to complete failure [5]. Among these disruptive elements, atomic oxygen (AO) from plasma is one of the dominant components, present in upper atmosphere, that badly influence the

degradation of coating materials [8]. Through space mission and ground based-simulation experiments, it has been observed that involved polymeric coatings and film shields undergoes dramatic degradation when exposed to AO plasma [9-12].

In the upper atmosphere, interaction of short wavelength solar UV radiation, (> 5.12 eV, < 243 nm) with molecular oxygen leads to the photo-disintegration and generate AO plasma [6,9]. However, exposure to AO is a peculiarly dependent upon the altitude of the spacecraft and the orientation history in LEO position. Moreover, AO is highly reactive and has dominant surface effects thereby, primarily, it oxidizes and removes the surface material. The mass loss depends upon the cumulative exposure of the AO. Since, AO exposure tends to erase the effects of previous surface damage, the extent of near-surface degradation can be correlated with the ratio of equivalent solar hours to AO exposure [11,13].

In recent years, a class of thermosetting polymer i. e. polyimide has emerged as a radiation protection blanket due to its exclusive properties such as flexibility, lightweight, inherent mechanical strength, robust temperature stability, excellent electric insulation, enormous UV stability, and remarkable infrared transparency [14,15].

However, in spite of the benefits of polyimide as a protective surface layer for the spacecraft, it's surface gets affected by the strong chemical reactions with the atomic oxygen species. Attempts to reduce the detrimental effects of atomic oxygen on the surface coatings of the spacecraft, therefore, still remains an area of investigation. Moreover, polyimide in combo with multilayered fluorinated polyethylene can readily provide solutions for insulation blankets for thermal control as well as low solar absorptance.

In literature, there have been few technical testing reports on design and development of anti-erosion (to atomic oxygen) coatings for providing protection to space vehicles on trial and testing basis [16]. There are a few reports on space environment exposure effects on ceramic based coatings for thermal protection systems [17]. More recently, nano-coated carbon-carbon structures have been found to be effective in reducing the detrimental effects of atomic oxygen for re-entry applications [18]. In another study, chemical vapor deposition based nano-coating of carbon composites for space materials for atomic oxygen shielding has been re-

ported [19]. Typically, silicon dioxide, fluoropolymer incorporated silicon dioxide, aluminum oxide, and germanium has been sputter deposited on polymers to provide protection against AO. Notably, large solar array blankets on the international space station have been coated with ~ 150 nm thick layer of SiO_2 for anti-erosion protection from AO. However, such coatings have a major drawback. The excess surface roughness may cause development of defects and stacking faults that allow AO to react and gradually undercut the protective coating layers [20]. By and large, paintings or coatings have several limitations in terms of surface bonding, peeling-off effects, scratching, friction/rubbing, wear/tear, etc., which may result into removal of coating, consequently, losing the protective paint. The purpose of this communication is to provide solutions to reduce atomic oxygen erosion of space quality polymeric coatings thereby modifying surface properties.

In the present work, doping of boron and fluorine (B/F) species into the surface region of polyimide up to a depth of ~ 2 μm using Co-60 γ -rays, has been found to be useful in reducing the surface erosion by atomic oxygen ions produced in laboratory plasma. Although ions have higher reactivity as compared to the neutral oxygen atoms, the relative comparison of the erosion rates for the doped surface vis-à-vis the virgin surface provides the usefulness of the treatment. The concentration and depth distribution of dopants in polyimide was analyzed using neutron depth profiling, Rutherford back scattering, energy dispersive x ray, and x-ray photoelectron spectroscopy [16]. The B/F doped polyimide vis-à-vis, the virgin counterpart were, exposed to mean value of 12 eV energetic AO ions, produced through electron cyclotron resonance (ECR) plasma system at different levels of fluencies. Erosion stability was investigated by number of techniques such as weight loss, vibration, and uv-visible spectroscopy as well as atomic force microscopy. By and large, the erosion yield was found to be reduced by almost 50%, as compared to the virgin sample, for the maximal B/F doped polyimide. Paper reports the details of the characteristic analysis of the B/F doped polyimide.

Experimental

Materials and Methods

The starting material used in the investigations was a polyimide film ($\text{C}_{22}\text{H}_{10}\text{N}_2\text{O}_7$, PMDA-ODA, Kapton-H, ©DuPont de Nemours, Inc., USA) which was made available by the Department of Space, Indian Space Research Organization (ISRO), Bangalore. Initially samples,

each of size 15 mm × 15 mm, were obtained by cutting a polyimide sheet of thickness ~ 50 μm. A large number of cut shards were kept ready for batch processing to characterize, doping, plasma treatment, post characterization, etc.

Radiation assisted doping of boron and fluorine (B/F) in polyimide

One of the crucial requirements was to dope polyimide with boron and fluorine atoms near surface region of the polyimide. For this purpose, solution of boron tri fluoride etherate (Grade: LR, Chemical formula: $(C_2H_5)_2O-BF_3$, concentration: 50 %, CAS: 109-63-07) was readily obtained from M/S Sigma Aldrich, USA. The prepared polyimide samples were kept in the glass bottles of diameter ~ 2.5 cm and height ~ 4 cm. The solution of BF_3 was poured into the bottles, ensuring of the complete immersion of polyimide samples into the solution. Six bottles were sealed and were subsequently kept in the Co-60 γ -rays irradiation chamber (energy: 1.173 and 1.332 MeV) for irradiation and accumulating the doses of 64, 96, 128, 192, 288 and 384 kGy, respectively, at room temperature.

Depth distribution in B/F polyimide: Neutron depth profiling (NDP), energy dispersive x-ray (EDS), and x-ray photoelectron spectroscopy (XPS)

The depth distribution of boron in polyimide was examined using the technique of Neutron Depth Profiling (NDP). The experimental method used was similar to that reported earlier for HDPE [21].

The presence of fluorine in polyimide was confirmed by EDS (Make: JEOL JSM 6360A JAPAN) and vis-à-vis compared using XPS. For XPS, the spectrum was recorded using Mg K_{α} (1253.6 eV) or Al K_{α} (1486.6 eV) x-rays with spectrometer resolution ~1.6 eV@ a pass energy ~ 50 eV. All XPS binding energy curves were calibrated with respect to C 1s binding energy curve @285 eV after making surface charging corrections. The concentration, C_s , of fluorine (relative%) in B/F polyimide were obtained after normalizing the intensity of each XPS peak with respect to the corresponding photoelectron cross-section. Notably, presence of fluorine in polyimide was also confirmed, previously, by Rutherford back scattering (RBS) technique, details of which are reported in our earlier communication [22].

Atomic oxygen plasma treatment: simulation of space radiation environment

Further, virgin, and all B/F polyimide were exposed to different fluencies of atomic oxygen ions from plasma. The plasma processing carried out in the present work was produced in an electron cyclotron resonance (ECR) plasma system [11,23] equipped with microwave cavity resonator in TE_{111} mode and a magnetron (power ~ 500 W, ω ~ 2.45 GHz) coupled to plasma chamber through waveguides. Figure 1 (a) shows the schematics of the system and (b) displays its photographic image during processing.

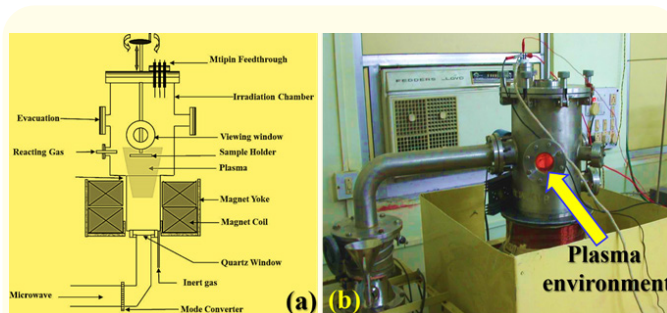


Figure 1: (a) Schematic representation of atomic oxygen ECR plasma system comprised of microwave injection, magnet, plasma chamber (including extraction ports), sample holder, plasma diagnostic probes, etc., and (b) photographic image of actual system while plasma processing.

During plasma processing, the base pressure was ~ 10^{-6} mbar and pure oxygen gas (99.9%) was introduced into the chamber through a mass flow meter. The experimental parameters such as the oxygen flow rate, microwave power, axial magnetic field, oxygen pressure, etc., were optimized in order to obtain stable ECR plasma. Importantly, the energy and the flux of oxygen ions in the ECR plasma at a certain position along the axis of the chamber and at different pressure conditions were measured using a three-grid retarding field analyzer (RFA) [11]. At the sample holder position, the energy ~ 12 eV and the flux ~ 5×10^{13} ions/cm²/s for the atomic oxygen ions were maintained at a given experimental parameters. The fluence of plasma ions was varied over ~ 5×10^{16} to 2×10^{17} ions/cm², from sample to sample, by varying the irradiation period.

Post plasma treatment characterizations

Virgin, B/F doped, and B/F doped and plasma treated polyimides were subsequently characterized using different tech-

niques, such as weight loss measurements, atomic force microscopy (AFM), Fourier transform infrared spectroscopy (FTIR) and uv-visible spectroscopy.

The weight loss measurements were performed by a microbalance with an accuracy of $\pm 1 \mu\text{g}$ before and after exposure to the AO ions. The variations in weight loss with the time of exposure has been analysed. The values of erosion (volume per atom) yields were determined from the expression given by: $E_y = \Delta M / (\rho \cdot A \cdot \Phi \cdot t)$, where, ΔM , is the change in mass of the sample, ρ is the density ($1.42 \text{ gm}\cdot\text{cm}^{-3}$ for polyimide), A is the area of the sample, Φ is the flux of incident oxygen ions and t is the time of exposure. The values of average erosion yield, E_y was determined to be $\sim 8.05 \times 10^{-22} \text{ cm}^3 \text{ atom}^{-1}$ for the virgin polyimide samples. The evaluated erosion rate of virgin polyimide for the AO ions is almost three order of magnitude higher than what universally reported for AO ($3 \times 10^{-24} \text{ cm}^3/\text{at}$). This is expected due to the higher activity and higher detrimental effects of ions as compared to the neutral atomic oxygen species.

AFM model (JEOL JSM 5200 JAPAN), studies were performed for probing the surface morphology. FTIR measurements were carried out to investigate the effect of irradiation on the molecular environment of polyimide. The measurements were performed using SHIMADZU 8400 FTIR spectrometer over $4000\text{-}350 \text{ cm}^{-1}$ with air as the reference. Moreover, for these samples the change in the band gap has been studied using the UV-visible spectroscopy (JASCO V-670 Spectrophotometer).

Results and Discussion

Doping of B/F in polyimide: depth distribution analysis

Figure 2 shows the variations in boron-concentration as a function of depth inside the sample of polyimide measured from the sample surface. Here, the depth- distribution with boron-concentration is deconvoluted from the recorded α -particle spectrum that gives values of concentration of boron atoms at different depths in a boron coated sample.

Three typical spectra are displayed for polyimide doped with B/F@64, 192, and 384 kGy of Gamma irradiation. By and large, each concentration profile had a mean value of the distribution at a certain depth (in μm) followed by a long diffusion tail. At the mean value, the concentration of ^{10}B is highest and trailing tails indicate

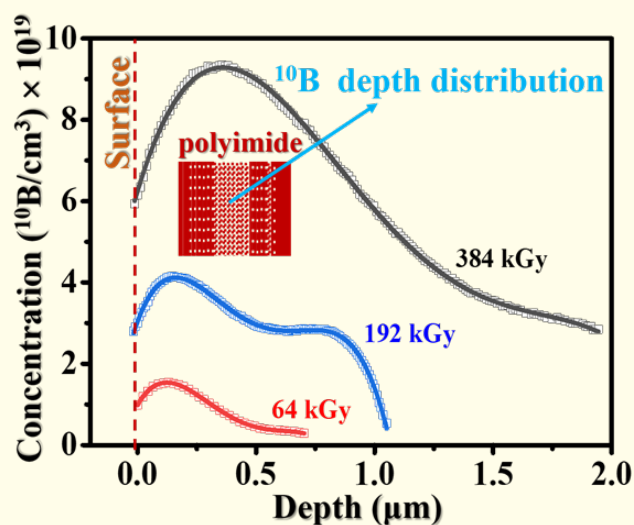


Figure 2: Concentration and depth distribution of ^{10}B in polyimide at various γ -ray dose. Inset shows schematics of radiation assisted diffusion of ^{10}B in polyimide.

the maximum penetration of the dopant in polyimide from the surface. We also note that, the diffusion has occurred from both the sides of polyimide surfaces. For B/F@64, the mean depth is noted at $\sim 0.4 \mu\text{m}$ and corresponding tail is seen to be extended upto $\sim 0.7 \mu\text{m}$. For B/F@192, mean depth and tail is noted, respectively at 0.15 and $1.0 \mu\text{m}$, whereas, for B/F@384, these values are, correspondingly observed at, 1.0 and $2.0 \mu\text{m}$. One can see that, the mean depth is skewed by one order of magnitude and range is extended, approximately, by three times from low to high value of the dose administered into polyimide. Notably, at lower doses the concentration of boron is more in the surface region as compared to the bulk. However, with increasing dose, the concentration in the bulk increases and on an average the concentration does not vary much with the depth. Unlike charge particles, γ -radiations have infinite value of penetration and no definite range in the material and, consequently, lead to different absorption mechanisms such as photoelectric, Compton, and pair production. However, for the combination of Co-60 γ -radiation energy ($E=1.173, 1.332 \text{ MeV}$) and carbonaceous ($Z=6$) polyimide the dominant mechanism is the Compton electron ejection, which is a probabilistic scattering process. This electron is responsible to cause segmental motions in polymeric chains by introducing voids in the material matrix to facilitate the atomic diffusion of boron and fluorine. The scattered γ -ray energy is given by:

Where, m_0 is ejected relativistic electron in rest mass unit (m_0c^2), θ , angle of scattered γ -ray, and, E_0 , energy of incident Co-60 γ -ray. Thus, by and large, figure 2 reveals that the concentration and depth of boron atoms in the polyimide samples increase with increasing dose of γ -radiations as measured using NDP technique.

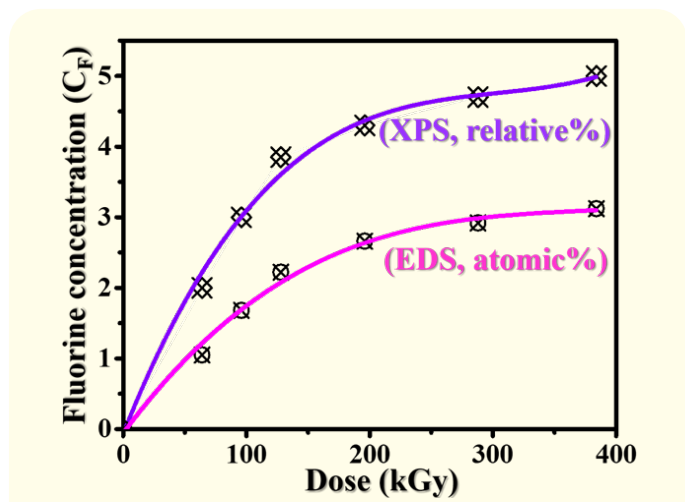


Figure 3: Variations in CF for B/F polyimide with dose of γ -rays; estimations using XPS and EDS.

Further, Figure 3 shows the variations in concentration of fluorine atoms (C_F) for B/F polyimide obtained by two surface sensitive techniques i. e. XPS and EDS. It is clear from both measurements that the amount of fluorine in polyimide has increased with increasing dose of irradiation. The Compton ejection of electron leads to induce dramatic variations in polyimide in terms of the processes containing chain scission and crosslinking. Among them, chain scissioning, mainly, dominates at low dose rates as compared with the high dose rates, administered by the energetic charge particles through accelerators. Such chain breaking generates segmental motions in polymeric chains and leads to the formation of appreciable number of radicals and disorder, in the form of discontinuities, chain bending, etc. This results into the modification in local free volume that allows radiation assisted diffusion of boron and fluorine in the polyimide matrix, as shown schematically in figure 4.

During irradiation, these atomic species diffuse through disordered zones produced in the surface region of polyimide and reside in such defect sites. Broadly, their diffusivity (rate of diffusion) de-

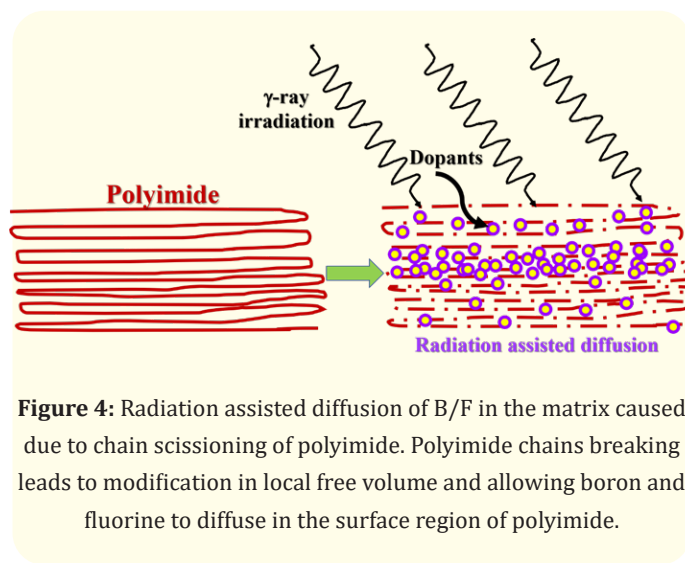


Figure 4: Radiation assisted diffusion of B/F in the matrix caused due to chain scissioning of polyimide. Polyimide chains breaking leads to modification in local free volume and allowing boron and fluorine to diffuse in the surface region of polyimide.

pends, mainly, upon the number of vacancies and defect sites that exist in the surface region. The results of the XPS revealed that in the diffused polyimide, the change in the oxygen concentration is marginal as compared with that of virgin polyimide on irradiation [20]. It is likely that the vacancies created by the emission of oxygen are filled with the oxygen atoms supplied during irradiation. In contrast, Mathakari, *et al.* [24] reported domination of crosslinking over scissioning at higher dose rate ~ 2000 kGy/h by exposing polyimide to 6 MeV electrons. In their case, enormous radiation density induced large zones of highly reactive free radicals were dynamically overlapping with each other, resulting into state of crosslinking, which is not the case in current studies.

The virgin and B/F polyimide material were exposed to AO to test their ability against erosion.

Atomic oxygen plasma treatment: simulation of LEO radiation environment

As discussed earlier, in the upper atmosphere, the AO gets evolved due to the dissociation of molecular oxygen on account of the solar UVs and that its energy depends on the speed, orientation, and position of the vehicle. Normally, the space vehicle receives an annual flux of AO in the range of 10^{19} - 10^{22} ions/cm² with mean energy of ~ 5 eV. Thus, during the mission period of the vehicle the thermal shield experiences an intense erosion and severe mass loss. Thus, ground-based simulation studies become important for

deciding the strategies to be chosen for architecting anti-erosion materials and coatings to fabricate the effective shielding materials.

Figure 5 (a) shows the variations in the weight loss (W_L in %), and (b) erosion yield (maximum) for virgin, and B/F polyimide at different γ -ray dose. From plot (a), it can be observed that the net loss in weight for virgin polyimide increases with increasing time of exposure to AO.

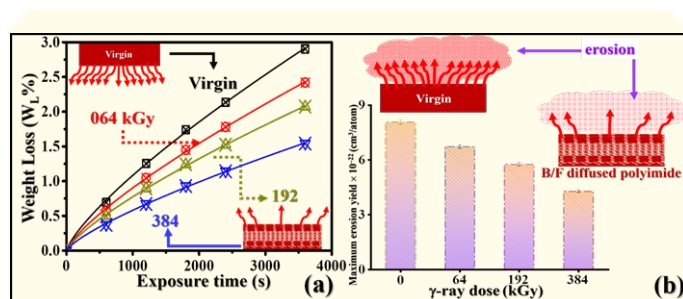


Figure 5: Variations in (a) % weight loss (W_L in %) with plasma exposure time (s) @ flux $\sim 5 \times 10^{13}$ ions/cm²/s, and (b) calculated maximum erosion yield for virgin and B/F polyimide at 64-384 kGy doses of γ -ray. Inset in (a) and (b) shows schematic representation of uncontrolled erosion in virgin, and B/F incorporated polyimide by AO.

However, for B/F polyimide the overall weight loss decreases with the increase in concentrations of boron and fluorine in the surface region of polyimide. One can see that the % change in weight of virgin polyimide is around 3% where as that for B/F@384 is ~ 1.5 % for maximum exposure up to 4000 s. Thus, almost double prevention in weight loss is noted. Other process which is reported relates to the chemical reactions of AO with near surface atoms to rupture the weak bonds. This results into the evolution of gaseous species from polymers during plasma treatment. The observed weight loss in polymer is therefore reported to be a combined effect of atoms which are removed from surface and redeposited onto surface during irradiation. For virgin polyimide, with interaction of AO, composition of carbon to nitrogen enriches almost twice due to loss of nitrogen that subsequently form new C-O-N binding with residual nitrogen species. But breakage of C-O-N bonding is also possible leading to creation of new species like NO_x onto surface that could be diffused out of the matrix. By and large, water vapor contamination and NO_x species could lead to the reduction in N

and O with enhancement in carbon in polyimide by AO. The lower weight loss for B/F polyimide, as compared to that in the virgin samples, can be attributed to the homogeneous and ordered dispersion of B-O in PI matrix as well as the formation of C-F bonds.

From plot (b), the maximum average erosion yield (E_y) is estimated to be $\sim 8.06 \times 10^{-22}$ cm³/atom for virgin and $\sim 4.28 \times 10^{-22}$ cm³/atom for B/F polyimide@384. The result, suggests the reduction of the magnitude of E_y by a factor of two, when compared with that for the virgin. The analysis has, therefore, revealed that the resistance to the attack by AO has been enhanced after diffusing boron and fluorine in the polymer- polyimide. This can be attributed to the bonding of the fluorine in B/F diffused surface of polyimide. It also appears that the emergence of C-F bonds resist the AO attack due to the endothermic chemical reaction, as shown, schematically, in figure 6.

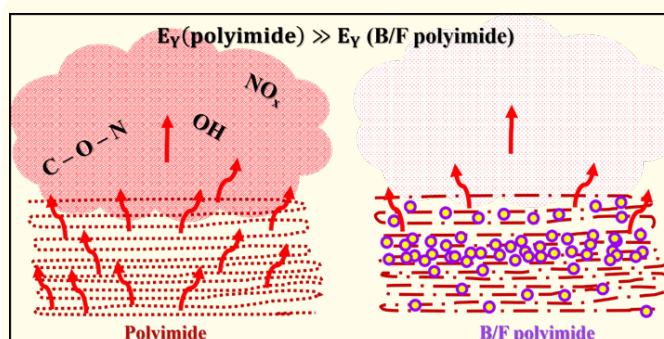


Figure 6: Schematics of erosion in polyimide by outgassing C-O-N, OH, and NO_x , there by enriching carbon in the matrix, whereas, B/F polyimide reduces erosion by a factor of two due to endothermic nature of C-F bond formation.

Further, 3D surface morphology of virgin, B/F polyimide has been investigated before and after exposure to the AO @ $\sim 2 \times 10^{17}$ ions/cm² up to 4000s and variations in topologies are shown in figure 7.

Figure 7(a) show surface condition of a typical virgin polyimide scanned for an area of $5 \times 5 \mu\text{m}^2$. The surface is seen to be quite smooth, however, at some places small hillock features (white arrows) are visible including line-faults (yellow arrows) due to the intrinsic polymeric chain erosion. By and large, the observed varia-

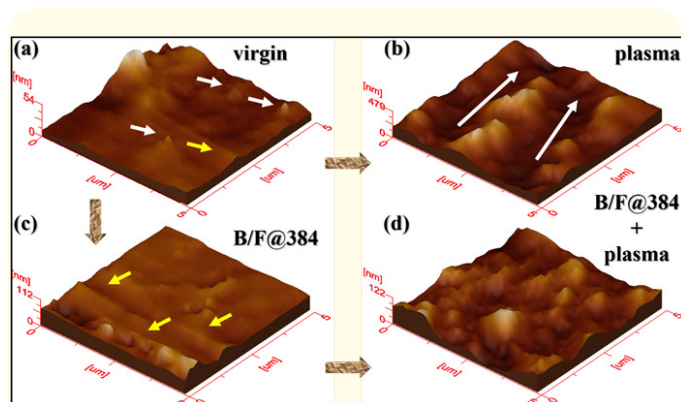


Figure 7: 3D surface topology recorded by AFM for (a) virgin, (b) plasma treated, (c) B/F polyimide at γ -ray dose of 384 kGy, and (d) B/F@384 treated with plasma. Plasma exposure time 4000 s. Typical scan area of $5 \times 5 \mu\text{m}^2$.

tions are attributed to the inherent composition emerged during fabrication of the polyimide film. The root mean square (rms) surface roughness is measured to be ~ 7 nm. Figure 7(c) displays the surface morphology of B/F polyimide (@ 384 kGy). The morphology is observed to be distinctly different with the reduction in small hill features and emergence of line-faults (yellow arrows). The rms surface roughness is calculated to be ~ 15 nm for B/F diffused polyimide. The values of rms surface roughness are observed to increase by almost two-fold with respect to that with the virgin sample. Figure 7 (b) shows the surface morphology of the virgin polyimide exposed to plasma. The dramatic variations are seen, particularly, the weak hillock features on the virgin surface became very prominent after plasma exposure, indicating range type pattern (shown by extended arrows). As discussed, virgin polyimide is prone to plasma sputtering of nitrogen, oxygen that are bonded weakly onto the surface polyimide chains. During plasma exposure these bonds get splashed from the surface and sub-surface region resulting into the modifications in the surface topology and causing redistribution of free volume available in the sub-surface region. It is also speculated that entire fault line might get eroded. From the three surface profiles (a), (b), and (c) it is revealed that changes in surface morphology for virgin surface is prominently more when directly exposed to oxygen plasma, whereas, for B/F doped polyimide, the changes are not that drastic. The rms surface roughness values calculated for plasma treated virgin polyimide is ~ 65 nm which is noted to be almost ten times higher than the calculated for the virgin rms values. However, on exposure of B/F polyimide

(@ 384 kGy) to the AO, it has marginal impact onto surface morphology. It seems that, presence of boron and fluorine in surface region of sample has reduced erosion as discussed earlier. And the obtained results are consistent with the weight loss and erosion yield analysis, presented before. The rms surface value of B/F polyimide exposed to AO is estimated to be ~ 18.2 nm which is closer to B/F polyimide.

In order to clarify the role of B/F in preventing erosion from plasma exposure, vibration spectroscopic analysis has been carried out for virgin and B/F polyimide, both exposed to plasma for 4000 s. Figure 8 shows the FTIR spectra for these specimens over $4000\text{-}1000 \text{ cm}^{-1}$.

There are seven functional imprints of PMDA-ODA that appears over $1000\text{-}4000 \text{ cm}^{-1}$. Their details are provided in Table 1 describing the functional groups, their characteristics and appearance in band.

Sr. No.	Group	Characteristic details	Band region (cm^{-1})
(i)	-C-O-	Stretching vibrations	1050-1250
(ii)	=C-N-	Cyclic imide (CO-N-CO)	1376-1390
(iii)	-C-C-	Skeleton benzene rings	1504
(iv)	-N-H-	Bending and stretching	1602 and 3486
(v)	-C=O-	Carbonyl stretching in PDMA	1724-1780
(vi)	-C-H-	Stretching	3085
(vii)	-O-H-	Stretching	3630

Table 1: Characteristic functional groups assigned for polyimide [25-27].

These functional groups are present in all samples. However, some changes have been observed, particularly, for skeleton ring stretching band (assigned as (iii) in Table 1) emerged at 1504 cm^{-1} . For virgin, the doublet at 1504 cm^{-1} is quite prominent that shows two vibration mode one breath in mode (Γ_1) and other breath out (ν_1). After plasma treatment, this peak is somewhat altered indicating modification in skeleton stretching band. For B/F@384 polyimide it is even changed with subsequent modification after plasma treatment.

Further we have also observed dramatic variations in absorption related to N-H bonds, both in bending and stretching modes.

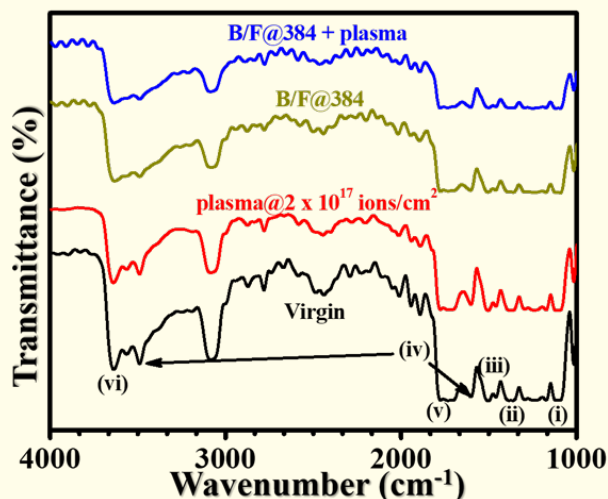


Figure 8: Recorded FTIR spectra for virgin, plasma @ 2×10^{17} ions/cm², B/F@ 384 kGy, and B/F@384, and plasma treated polyimide.

Especially, N-H stretching seems to have lost its symmetry after plasma processing. By and large, for virgin, more chain scissioning has been seen as compared with B/F polyimide after plasma treatment. This can be confirmed by a closer observation in terms of dramatic decrease in intensities of almost all peaks after plasma irradiation of virgin. While the reduction in overall IR intensities for functional peaks is marginal for B/F polyimide after AO exposure at a fluence of $\sim 2 \times 10^{17}$ ions/cm². The decrease in the intensities of the peaks reveals that the concentration of the corresponding bonds has lowered due to the ejection of atoms at the corresponding elements from the surface. These results, therefore, indicate that the surface of the boron and fluorine diffused polyimide samples become more resistant to the AO attack.

Figure 9 (a) shows the UV-visible spectra for virgin, and plasma treated polyimide @ 5×10^{16} and 2×10^{17} ions/cm². It is observed that, in the wavelength range between 500 to 900 nm, there is a significant reduction in the % transmittance due to plasma treatment at various ion fluences. Particularly, at high value of plasma fluence the transmittance beyond 550 nm is observed to vary between 20-30%. Figure 9(b) shows transmittance spectra for B/F diffused polyimide@384 kGy γ -ray dose. It is worth noticing that there is no significant change in the absorption edge for both, virgin and plasma treated polyimide. Consequently, the band gap of

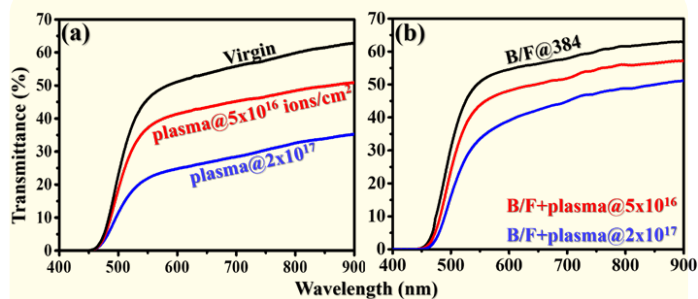


Figure 9: UV-Visible transmission spectra recorded for: (a) virgin, plasma treated (@ 5×10^{16} and 2×10^{17}) polyimide, and (b) B/F diffused@384 kGy with sequential plasma treatment @ 5×10^{16} and 2×10^{17} ions/cm².

polyimide sample, even after B/F doping has remained unaltered. Moreover, the reduction in transmittance level beyond 550 nm is not seen to be too drastic when compared with virgin polyimide treated with AO. For highest plasma fluence @ 2×10^{17} ions/cm² for B/F diffused@384 kGy the change in the transmittance level is recorded to be between 30-40% in the range of 550-900 nm. The overall prevention of loss in B/F polyimide shows protection from AO plasma degradation due to presence of boron, carbonization, and C-F bonding. The results presented herein are internally consistent [28].

Our study has thus provided a solution towards fabricating a facile material- architecture by diffusing boron and fluorine into polyimide. Such a fabrication can provide an effective anti-erosion coating for AO plasma environment which the space vehicle experience during their mission period in LEO.

Conclusion

In conclusion, we have designed and tested a prototype anti-erosive coating that are importantly required for space radiation protection, particularly, at an altitude of communication satellite range. Initially, polyimide ($C_{22}H_{10}N_2O_7$, PMDA-ODA, Kapton-H) was subjected to radiation assisted doping of boron and fluorine (B/F polyimide) over the dose, ranging between 64 to 384 kGy. These samples were subjected to surface measurements like neutron depth profiling, energy dispersive x-ray, and x-ray photoelectron spectroscopy to investigate the depth/concentration distribution, and bonding within the matrix. Details of the analysis are pre-

sented. However, in a nutshell, we have revealed that, with subsequent increase in the amount of dose, boron was diffused upto $\sim 2 \mu\text{m}$, whereas, fluorine concentration was found to be 5% (max.) bonded with carbonaceous backbone of polyimide. Virgin and B/F doped polyimide was subjected to AO treatment using ECR based plasma excited by microwave source, with a power $\sim 500 \text{ W}$, $\omega \sim 2.45 \text{ GHz}$. The mean energy of the ions was around 12 eV and having capability to deliver ion flux of $5\text{-}20 \times 10^{16} \text{ ions/cm}^2$. Both types of polyimides were analyzed for % weight loss, erosion yield, topography, vibrational absorption, and UV visible transmittance. The weight loss measurement showed prevention of mass loss by at least three-fold for highest B/F doped polyimide, whereas, erosion yield was reduced by a factor of two. Although the erosion yield of AO ions is observed to be higher by three orders of magnitude for polyimide as compared to that reported [17-19] for AO atoms, the relative improvement of the radiation resistance of the BF doped polyimide surfaces to the attack of AO will remain the same. This proves the improved erosion resistance property of the treated surface against AO in space applications. The AO enriches carbon surface of polyimide there-by outgassing nitrogen, oxygen, hydrogen resulting unprecedented erosion losses. However, presence of boron and fluorine in the backbone of polyimide prevent the attack of atomic oxygen due to C-F bonding and its endothermic characteristic. Possible mechanism is discussed.

Acknowledgement

The financial support for this work was received from the Department of Science and Technology, New Delhi, under a project and is gratefully acknowledged. One of authors (RM) is grateful to the Govt. of Yemen for the financial assistance and other support which enabled him to carry out research work at the University of Pune, Pune (India).

Bibliography

- Mittal KL. "Polyimides and Other High Temperature Polymers: Synthesis, Characterization and Applications". *CRC Press* 2 (2003).
- Tribble AC. "The space environment: implications for spacecraft design-revised and expanded edition". Princeton University Press (2020).
- Skurat VE., *et al.* "Proceedings of the Sixth International Symposium on Materials in a Space Environment ESTES, Noordwijk, The Netherlands". 19-23 September (1994): 183-187.
- Wolan JT and Hoflund GB. "Chemical and structural alterations induced at Kapton® surfaces by air exposures following atomic oxygen or 1 keV Ar+ treatments". *Journal of Vacuum Science and Technology A: Vacuum, Surfaces, and Films* 17.2 (1999): 662-664.
- Milinchuk VK., *et al.* "Degradation of polymer materials in low earth orbits". *High Energy Chemistry* 38.1 (2004): 8-12.
- Packirisamy S., *et al.* "Atomic oxygen resistant coatings for low earth orbit space structures". *Journal of Materials Science* 30.2 (1995): 308-320.
- Katz I., *et al.* "Plasma turbulence enhanced current collection: Results from the plasma motor generator electrodynamic tether flight". *Journal of Geophysical Research: Space Physics* 100.A2 (1995): 1687-1690.
- Minton T K and Garton DJ. "Dynamics of atomic-oxygen-induced polymer degradation in low earth orbit". In *Chemical dynamics in extreme environments* (2001): 420-489.
- De Groh K K and Banks BA. "Atomic oxygen erosion data from the MISSE 2-8 missions (No. NASA/TM—2019-219982)" (2019).
- Osborne J J., *et al.* "Satellite and rocket-borne atomic oxygen sensor techniques". *Review of Scientific Instruments* 72.11 (2001): 4025-4041.
- Abdul Majeed RM., *et al.* "Irradiation effects of 12 eV oxygen ions on polyimide and fluorinated ethylene propylene". *Radiation Effects and Defects in Solids* 161.8 (2006): 495-503.
- Zhao XH., *et al.* "A study of the reaction characteristics and mechanism of Kapton in a plasma-type ground-based atomic oxygen effects simulation facility". *Journal of Physics D: Applied Physics* 34.15 (2001): 2308.
- Tagawa M and Yokota K. "Issues and consequences of space environmental effect on materials". *Transactions of the Japan society for aeronautical and space sciences, space technology Japan* 7.26 (2006): Tr_2_21-Tr_2_26.

14. Wu Z., *et al.* "Preparation of surface conductive and highly reflective silvered polyimide films by surface modification and in situ self-metallization technique". *Thin Solid Films* 493.1-2 (2005): 179-184.
15. Tahara H., *et al.* "Exposure of space material insulators to energetic ions". *Journal of Applied Physics* 78.6 (1995): 3719-3723.
16. Tomczak SJ., *et al.* "Properties and improved space survivability of poss (polyhedral oligomeric silsesquioxane) polyimides". *MRS Online Proceedings Library (OPL)* (2004): 851.
17. Pastore R., *et al.* "Space environment exposure effects on ceramic coating for thermal protection systems". *Journal of Spacecraft and Rockets* 58.5 (2021): 1387-1393.
18. Delfini A., *et al.* "Evaluation of atomic oxygen effects on nano-coated carbon-carbon structures for re-entry applications". *Acta Astronautica* 161 (2019): 276-282.
19. Delfini A., *et al.* "CVD nano-coating of carbon composites for space materials atomic oxygen shielding". *Procedia Structural Integrity* 3 (2017): 208-216.
20. Abdul Majeed RMA., *et al.* "Dielectric constant and surface morphology of the elemental diffused polyimide". *Journal of Physics D: Applied Physics* 39.22 (2006): 4855.
21. Dokhale P A., *et al.* *Materials Science and Engineering B* 57 (1998): 1-8.
22. Briggs D. "Practical surface analysis". Auger and X-Ray Photoelectron Spectroscopy 1 (1990): 151-152.
23. Abdul Majeed RMA., *et al.* *Nuclear Instruments and Methods in Physics Research B* 490 (2021): 49-54.
24. Mathakari NL., *et al.* "6 MeV pulsed electron beam induced surface and structural changes in polyimide". *Materials Science and Engineering: B* 168.1-3 (2010): 122-126.
25. Youmei Sun., *et al.* *Nuclear Instruments and Methods in Physics Research B* 218 (2004): 318.
26. Naddaf M., *et al.* "Surface interaction of polyimide with oxygen ECR plasma". *Nuclear Instruments and Methods in Physics Research Section B: Beam Interactions with Materials and Atoms* 222.1-2 (2004): 135-144.
27. Severin D., *et al.* "Degradation of polyimide under irradiation with swift heavy ions". *Nuclear Instruments and Methods in Physics Research Section B: Beam Interactions with Materials and Atoms* 236.1-4 (2005): 456-460.
28. Sun Y., *et al.* "The thermal-spike model description of the ion-irradiated polyimide". *Nuclear Instruments and Methods in Physics Research Section B: Beam Interactions with Materials and Atoms* 218 (2004): 318-322.